Research Square

Preprints are preliminary reports that have not undergone peer review.
They should not be considered conclusive, used to inform clinical practice,
or referenced by the media as validated information.

Aflatoxin B_1 reduction on spiked maize and wheat by an ambient-air Tesla-coil discharge: biphasic time course, input-current effect and the gap to the East African limit

Nicodemus Masunzu
The Nelson Mandela African Institution of Science and Technology (NM-AIST)
Musa Chacha
The Nelson Mandela African Institution of Science and Technology (NM-AIST)
Jofrey Raymond
jofrey.raymond@nm-aist.ac.tz

The Nelson Mandela African Institution of Science and Technology (NM-AIST)

Research Article

Keywords: Aflatoxin B1, Atmospheric-pressure plasma, Weibull kinetics, Maize, Wheat, Regulatory limit

Posted Date: November 12th, 2026

DOI: https://doi.org/10.21203/rs.3.rs-11533555/v1

License: This work is licensed under a Creative Commons Attribution 4.0 International License.
Read Full License

Additional Declarations: No competing interests reported.

Abstract

Grain above aflatoxin limits needs a reagent-free decontamination step that runs near ambient temperature. This study quantified the reduction of aflatoxin B_1 (AFB_1) on spiked maize and wheat exposed to an atmospheric-pressure air discharge from a solid-state Tesla-coil point electrode and translated the result into regulatory terms. Grain portions of 50 g were spiked with AFB_1, treated at input currents of 2 and 4 A for 10–30 min, and analysed by HPLC with fluorescence detection; every combination was run in triplicate. Pooled mean reduction was 65.2% (95% CI 63.4–67.0%) at 2 A and 78.6% (76.8–80.4%) at 4 A, and 68.9%, 74.5% and 79.8% after 10, 20 and 30 min, with reduction levelling beyond 30 min. Both factors were significant (current, $F(1,24) = 131.9$; time, $F(2,34) = 47.2$; both $p < 0.001$). The time course was biphasic: a Weibull model fitted to the pooled means gave a shape parameter of 0.28 (95% interval 0.22–0.33), and a two-fraction description assigned 61% of the toxin to a rapidly reduced, surface-accessible fraction and the remainder to a shielded fraction reduced at 0.022 min^{-1}. At the 30 min mean, a single treatment brings grain starting at up to about 25 µg/kg to the East African limit of 5 µg/kg; the median contamination of 24 µg/kg in Tanzanian home-stored maize lies within this range, whereas lots at 158–2351.5 µg/kg require 96.8–99.8% reduction. Ambient-air plasma is therefore a compliance step for moderately contaminated grain and one stage of combined control for heavily contaminated lots.

Introduction

Aflatoxin B_1 (AFB_1), produced mainly by *Aspergillus flavus* and *A. parasiticus*, is a Group 1 human carcinogen (IARC Working Group on the Evaluation of Carcinogenic Risks to Humans 2012). Hepatic cytochrome P450 enzymes, chiefly CYP1A2 and CYP3A4, oxidise the C8 = C9 vinyl ether double bond of its terminal furan ring to the AFB_1-*exo*-8,9-epoxide, which forms N7-guanine DNA adducts (Kensler et al. 2011). Aflatoxin accounts for an estimated 4.6–28.2% of hepatocellular carcinoma cases worldwide (Liu and Wu 2010) and is associated with growth impairment in children (Khlangwiset et al. 2011). In Tanzania, biomarker data attribute about 1,480 new liver cancer cases in 2016 to aflatoxin (Kimanya et al. 2021).

Dietary exposure in Tanzania spans a wide range. Biomarker-based estimates of aflatoxin intake ranged from 15.0 to 10,926.0 ng/kg body weight per day, with a median of 105.5 ng/kg body weight per day (Kimanya et al. 2021), and maize is the principal vehicle because it is eaten daily and in large amounts. Because exposure scales with the concentration in the grain consumed, any step that lowers the AFB_1 content of a lot lowers the dose received from it in the same proportion. A decontamination step that can be applied after harvest, at the point where grain is stored or milled, therefore acts directly on the quantity that drives the health burden.

Contamination of the maize supply is both frequent and highly variable. In rural Tanzanian households, aflatoxins were detected in 18% of home-stored maize samples, at a median of 24 µg/kg and a maximum of 158 µg/kg, and 12% of samples exceeded the national limit for total aflatoxins of 10 µg/kg

(Kimanya et al. 2008). In Mtwara region, 71.1% of maize grain samples exceeded the East African Community limits, with a maximum AFB_1 concentration of 2351.5 µg/kg (Gichohi-Wainaina et al. 2023). The East African standard sets 5 µg/kg for AFB_1 and 10 µg/kg for total aflatoxins in maize grain (East African Community 2011), and the European Union applies 2 and 4 µg/kg to cereals for direct human consumption (European Commission 2023). Grain that fails these limits leaves formal trade, and a large share is consumed in the household.

Sorting, cleaning and milling lower mean contamination, and chemical treatments degrade aflatoxins under alkaline or oxidising conditions, but physical methods depend on visibly damaged kernels and chemical methods require reagents, heat and regulatory acceptance of reaction products (Karlovsky et al. 2016; Hojnik et al. 2017). Cold atmospheric plasma acts without reagents: electrical discharges in humid air produce reactive oxygen and nitrogen species, including atomic oxygen, hydroxyl radicals, ozone and nitrogen oxides, at near-ambient gas temperature (Misra et al. 2019; Gavahian and Cullen 2020; Javed et al. 2025). In AFB_1, plasma species cleave the C8 = C9 double bond, the site of metabolic activation, and the products lose cytotoxicity and genotoxicity (Hojnik et al. 2021b; Shi et al. 2017b). On cereals, high-voltage atmospheric plasma reduced aflatoxin in corn by 62% and 82% after 1 and 10 min (Shi et al. 2017a), cold atmospheric plasma reduced AFB_1 in maize by up to 66% (Wielogorska et al. 2019), and low-pressure nitrogen plasma reduced aflatoxin in naturally contaminated maize by 82.6% (Kamano et al. 2025).

Two questions limit the use of these results in grain stores. The first concerns the time course. Percentage reductions are usually reported at single conditions, yet degradation of mycotoxins slows when the toxin is embedded in a matrix (ten Bosch et al. 2017), and aflatoxin reduction on corn under high-voltage plasma follows a non-log-linear, logistic course (Shi et al. 2017a). Whether the reduction on grain approaches a ceiling, and at what level, determines how much a longer exposure can deliver. The second concerns regulation: a percentage reduction becomes a management tool when it is set against the contamination levels found in the field and the limits that apply to them. Many effective sources also depend on argon, nitrogen or reduced pressure (Park et al. 2007; Siciliano et al. 2016; Kamano et al. 2025), which are difficult to supply in rural East Africa.

This study therefore asked how AFB_1 reduction on maize and wheat under an ambient-air discharge depends on input current and exposure time, what form the time course takes, and which field contamination levels a single treatment brings within the East African and European limits. The aims were to (i) quantify the effects of input current and exposure time; (ii) describe the time course with kinetic models and separate a surface-accessible from a shielded toxin fraction; and (iii) express the result as the range of starting contamination that one treatment brings into compliance.

Materials and methods

Plasma source

Grain was treated in PGM-SE1, a single-resonant solid-state Tesla-coil generator that sustains an atmospheric-pressure discharge in ambient air from a point electrode above a grounded plane inside a 0.5 L glass chamber; its design, construction and operating window are reported separately (Masunzu et al. submitted). Input current was set with a variac and read on the generator's analogue ammeter.

Grain and AFB spiking

Maize and wheat grains were purchased from local markets and cleaned to remove impurities. Grain (50 g) was spiked with an AFB_1 solution (25 µg/mL in acetonitrile), distributed evenly over the grain and mixed for uniform contamination, then dried under laminar airflow to a moisture content of 13–14%, measured with a calibrated grain moisture meter, and kept in sealed containers at ambient conditions until treatment.

Plasma treatment

Samples were placed on a non-conductive tray inside the plasma chamber, the detachable lid was closed, and the discharge was run with ambient air as the working gas. The factors were input current (2 and 4 A), exposure time (10, 20 and 30 min) and electrode–sample distance (2 and 4 cm); each combination was run three times. The generator was calibrated before each run. Untreated spiked grain served as the control, procedural blanks of unspiked grain passed through the same handling and analysis, and environmental blanks were included in each run. The effect of electrode–sample distance belongs to the characterisation of the generator and is reported with it; here, current and time means are pooled over the two distances.

Each treatment followed the same sequence. The chamber and tray were cleaned and inspected, the generator was calibrated and its coil alignment checked, and the spiked portion was placed on the tray at the set electrode–sample distance. The lid was closed, the input current was set with the variac and confirmed on the ammeter, and the discharge was run for the set time while the steady bluish glow of the plasma was observed through the glass; any change in plasma intensity or colour was recorded and corrected. After treatment the sample was removed, sealed and stored for analysis, and the chamber and tray were cleaned before the next run. Temperature, humidity and atmospheric pressure in the laboratory were recorded for each run, and the laboratory was ventilated throughout to disperse ozone and other reactive by-products.

The design is a full factorial of input current (two levels), electrode–sample distance (two levels) and exposure time (three levels), with three replicate runs of every combination. Each factor level is therefore represented across all levels of the other two factors, and its marginal mean averages over them. This structure is what allows the effect of current to be read across all times and distances, and the effect of time across both currents and distances. The reduction of each replicate was computed against the

untreated spiked control of the same series, and the marginal means, SD and 95% CI were formed from these replicate reductions.

AFB_1 determination

AFB_1 was determined by the standard method for maize, AOAC Official Method 991.31 (Trucksess et al. 1991). Treated grain was ground to a fine powder and extracted with methanol–water (80:20, v/v); the extract was filtered, diluted and cleaned up on an AFB_1-specific immunoaffinity column, from which AFB_1 was eluted with methanol. The eluate was analysed by high-performance liquid chromatography with fluorescence detection (HPLC-FLD) on a C18 column with acetonitrile–water (25:75) as mobile phase at 1.0 mL/min, with post-column photochemical derivatisation to enhance AFB_1 fluorescence, as in EN 14123 (European Committee for Standardization 2007), and detection at 360 nm excitation and 450 nm emission. AFB_1 was quantified by external calibration with a certified AFB_1 standard, with standard solutions analysed alongside the samples and replicate analyses for each sample. Reduction was calculated as $(1 - C_t/C_0) \times 100$, where C_0 is the concentration in the untreated spiked control and C_t the concentration after treatment. Untreated spiked controls were extracted and analysed identically to the treated grain, so that extraction recovery cancels in the ratio C_t/C_0 and the calculated reduction reflects the plasma exposure. Procedural blanks tested the handling and analysis for contamination or bias, and environmental blanks in each run tested for contamination from external sources.

Statistical analysis

Results are reported as marginal means with SD and 95% confidence intervals (CI), each pooled over the other factors of the factorial series. Group sizes were derived from the reported standard deviations and 95% confidence intervals, and tests were recomputed from summary statistics (Welch's t-test; one-way ANOVA with Tukey–Kramer comparisons) (Larson 1992). The group size n of each marginal mean was obtained from $n = (t_{0.975,\,n-1} \cdot SD/h)^2$, where h is the half-width of the 95% CI, solved iteratively and rounded to the nearest integer. The effect of input current was tested by Welch's t-test and one-way ANOVA, $F(1, N - 2)$; the effect of exposure time by one-way ANOVA, $F(2, N - 3)$, with Tukey–Kramer pairwise comparisons. Effect sizes are Cohen's d with the pooled SD, with 95% CI from its large-sample standard error, and η^2 for exposure time, with a 95% CI from the noncentral F distribution. The significance level was 0.05.

Kinetic models

Two models were fitted to the pooled time means, with the untreated control defining $C_t/C_0 = 1$ at $t = 0$. The Weibull model (Mafart et al. 2002), $\log_{10}(C_t/C_0) = -(t/\delta)^p$, was fitted by linear regression of $\log_{10}[-\log_{10}(C_t/C_0)]$ on $\log_{10} t$, where p is the shape parameter ($p < 1$ indicates a decelerating, tailing course) and δ the time for the first decimal reduction. A two-fraction model, $C_t/C_0 = f \cdot \exp(-k_1 t) + (1 - f) \cdot \exp(-k_2 t)$, describes a surface-accessible fraction f reduced rapidly and a shielded fraction $(1 - f)$ reduced at

k_2; because the accessible fraction was exhausted within the first 10 min, k_2 and f were obtained from a log-linear fit over 10–30 min. Uncertainty was propagated by Monte Carlo resampling (20,000 draws) of each time mean from a normal distribution with standard error SD/√n, using the derived group sizes; reported intervals are the 2.5th and 97.5th percentiles. These models describe pooled marginal means and are used to characterise the shape of the time course.

Regulatory analysis

For a starting concentration C_0 and a limit L, the reduction required is $100(1 - L/C_0)$, and the highest starting concentration brought to L by a reduction R is $L/(1 - R/100)$. Because both relations are ratios, they hold for any starting concentration, provided the fractional reduction is independent of the starting level over the range considered; this condition is standard for surface reactions in which the toxin is far from saturating the supply of reactive species. These relations were evaluated for the 30 min mean (79.8%, 95% CI 78.2–81.4%) and for the upper end of the grain range (85%), against the East African AFB_1 limit of 5 µg/kg (East African Community 2011) and the European limit of 2 µg/kg (European Commission 2023), at contamination levels reported for Tanzanian maize (Kimanya et al. 2008; Gichohi-Wainaina et al. 2023). All calculations were made in Python with SciPy 1.13 (Virtanen et al. 2020). AI-based coding tools assisted in preparing the analysis and figure scripts; the authors checked each output against the source data.

Results

Input current and exposure time

Both factors raised AFB_1 reduction (Table 1; Fig. 1). Pooled over exposure time and electrode–sample distance, reduction was 65.2 ± 3.1% at 2 A (n = 14) and 78.6 ± 2.8% at 4 A (n = 12), a difference of 13.4 percentage points (95% CI 11.0–15.8; Welch's $t(23.9) = 11.6$; $F(1,24) = 131.9$, $p < 0.001$) and a Cohen's d of 4.5 (95% CI 3.1–6.0). Pooled over current and distance, reduction was 68.9 ± 2.7% (n = 12), 74.5 ± 3.0% (n = 13) and 79.8 ± 2.5% (n = 12) after 10, 20 and 30 min. Exposure time had a significant effect (one-way ANOVA, $F(2,34) = 47.2$, $p < 0.001$) and explained 74% of the variance among time groups ($\eta^2 = 0.74$, 95% CI 0.54–0.81). In Tukey–Kramer comparisons, each 10 min step added 5.6 (95% CI 2.9–8.3) and 5.3 (2.6–8.0) percentage points, and the 10–30 min span added 10.9 points (8.1–13.7); all three differences were significant ($p < 0.001$), with d = 2.0 (1.0–2.9), 1.9 (1.0–2.9) and 4.2 (2.8–5.6). Across individual grain conditions, reduction ranged from 60% to 85%, and reduction levelled off at exposure times beyond 30 min.

Table 1
AFB_1 reduction on spiked maize and wheat by input current and exposure time: marginal means, group sizes and effect sizes

Factor	Level	Mean (%)	SD	95% CI (%)	n	Difference vs reference (95% CI)	Cohen's d (95% CI)
Input current	2 A (reference)	65.2	3.1	63.4–67.0	14	–	–
	4 A	78.6	2.8	76.8–80.4	12	+ 13.4 (11.0–15.8)	4.5 (3.1–6.0)
Exposure time	10 min (reference)	68.9	2.7	67.2–70.6	12	–	–
	20 min	74.5	3.0	72.7–76.3	13	+ 5.6 (2.9–8.3)	2.0 (1.0–2.9)
	30 min	79.8	2.5	78.2–81.4	12	+ 10.9 (8.1–13.7)	4.2 (2.8–5.6)

Means, SD and 95% CI from the factorial dataset, pooled over the other factors. n is derived from the SD and 95% CI. Current, Welch's t-test and $F(1,24) = 131.9$; exposure time, $F(2,34) = 47.2$, $\eta^2 = 0.74$; both $p < 0.001$. Difference CIs: Welch for current, Tukey–Kramer for time.

Figure 1 presents the two factors side by side on a common scale. The current effect in panel a is larger than any single time step in panel b, and the boxes of the 95% CI at 2 and 4 A are separated by almost 10 percentage points. In panel b the course from the untreated control to the first measurement is steep, and the three measured means then rise along a much flatter line. The visual contrast between the steep first segment and the flat later segments is the observation that the kinetic models quantify.

A biphasic time course

The time course did not follow a single exponential from zero. An apparent first-order constant calculated from the origin fell from 0.117 min^{-1} at 10 min to 0.068 min^{-1} at 20 min and 0.053 min^{-1} at 30 min, a fall that identifies a rapid initial phase followed by a slower one. The Weibull model described the three means closely (fitted 68.5%, 75.4% and 79.2% against observed 68.9%, 74.5% and 79.8%) with a shape parameter $p = 0.28$ (95% interval 0.22–0.33), well below 1, and a first-decimal-reduction time δ = 117 min (85–187 min) (Fig. 2). In the two-fraction description, the accessible fraction was $f = 0.61$ (0.58–0.64), removed within the first 10 min, and the shielded fraction of 0.39 decayed at $k_2 = 0.022$ min^{-1} (0.017–0.026 min^{-1}), a half-life of 32 min; the fitted values were 68.7%, 74.8% and 79.7%. The two models agree that the second phase removes the shielded fraction slowly, and the levelling of reduction beyond 30 min marks the practical ceiling of a single exposure at these settings.

The parameters of both descriptions are collected in Table 2. The Weibull fit reproduces the three time means within 0.6 percentage points, and the two-fraction fit within 0.3 points, so both describe the measured course to within its confidence limits. They differ in what they extrapolate: the Weibull curve

continues to decline slowly beyond 30 min, whereas the two-fraction description attributes the late decline to a single slow pool. The reported levelling of reduction beyond 30 min is closer to the second picture, with part of the shielded pool effectively out of reach of the discharge.

Table 2
Kinetic descriptions of the pooled time course of AFB_1 reduction on spiked grain

Model	Parameter	Estimate	95% interval	Fitted reduction at 10, 20, 30 min (%)
Apparent first order from t = 0	k at 10; 20; 30 min (min^{-1})	0.117; 0.068; 0.053	–	Exact at each point
Weibull	Shape p	0.28	0.22–0.33	68.5; 75.4; 79.2
	First 1-log time δ (min)	117	85–187	
Two-fraction	Accessible fraction f	0.61	0.58–0.64	68.7; 74.8; 79.7
	Slow-phase k_2 (min^{-1})	0.022	0.017–0.026	
	Slow-phase half-life (min)	32	–	

Observed means: 68.9%, 74.5% and 79.8%. Intervals from Monte Carlo resampling with standard error SD/√n. All values derived from the pooled marginal means.

Starting levels brought into compliance

A reduction of 79.8% leaves 20.2% of the starting concentration. A single 30 min treatment therefore brings grain starting at up to 24.8 µg/kg to the East African AFB_1 limit of 5 µg/kg, and up to 9.9 µg/kg to the European limit of 2 µg/kg (Fig. 3; Table 3). Over the 95% CI of the 30 min mean, the East African break-even lies between 22.9 and 26.9 µg/kg, and at the upper end of the grain range (85%) it rises to 33.3 µg/kg. The pooled 4 A mean of 78.6% corresponds to 23.4 µg/kg, and the pooled 2 A mean of 65.2% to 14.4 µg/kg. Against field data, the median of 24 µg/kg reported for contaminated home-stored maize in rural Tanzania (Kimanya et al. 2008) falls at the break-even and would be reduced to 4.8 µg/kg. Lots at 158 µg/kg, the maximum of the same survey, require 96.8% reduction, and lots at 2351.5 µg/kg, the Mtwara maximum (Gichohi-Wainaina et al. 2023), require 99.8%. A lot at 500 µg/kg would retain about 101 µg/kg after the 30 min mean reduction and requires 99.0% to meet the East African limit.

Table 3
Reduction required to reach the East African AFB_1 limit (5 µg/kg) and residual concentration after a single treatment, for starting levels from Tanzanian surveys

Starting level (µg/kg)	Basis	Reduction required (%)	Residual at 79.8% (µg/kg)	Residual at 85% (µg/kg)	Meets 5 µg/kg
10	Tanzanian total aflatoxin limit	50.0	2.0	1.5	Yes
24	Median, home-stored maize (Kimanya et al. 2008)	79.2	4.8	3.6	Yes, at break-even
33.3	Break-even at 85%	85.0	6.7	5.0	At 85%
158	Maximum, home-stored maize (Kimanya et al. 2008)	96.8	31.9	23.7	No
500	Heavily contaminated lot	99.0	101.0	75.0	No
2351.5	Maximum, Mtwara maize (Gichohi-Wainaina et al. 2023)	99.8	475.0	352.7	No

Required reduction = $100(1 - 5/C_0)$; residual = $C_0(1 - R/100)$. Survey values from Kimanya et al. (2008) are total aflatoxins; the calculation applies the AFB_1 reduction to them. 79.8%, 30 min pooled mean; 85%, upper end of the grain range.

Table 3 reads row by row as a triage scheme. Grain at twice the East African limit (10 µg/kg) needs half its AFB_1 removed and is brought to 2.0 µg/kg, below even the European limit. Grain at the Tanzanian median of 24 µg/kg needs 79.2% and is brought to 4.8 µg/kg at the 30 min mean, so it sits at the edge of compliance and depends on the treatment reaching at least the mean. At 33.3 µg/kg the required reduction equals the 85% upper end of the grain range. Above that level, at 158, 500 and 2351.5 µg/kg, the residuals of 31.9, 101.0 and 475.0 µg/kg remain well above the limit, and these lots fall outside what a single exposure can deliver.

Discussion

An ambient-air discharge reduced AFB_1 on spiked maize and wheat by up to 85%, with a biphasic time course in which most of the toxin was removed within 10 min and the remainder was removed slowly, and a single 30 min treatment brought grain starting at up to about 25 µg/kg within the East African limit. The sections below explain the two phases, compare the result with published plasma treatments and set out the routes to compliance for more heavily contaminated grain.

Surface-accessible and shielded toxin

A Weibull shape parameter of 0.28 and an accessible fraction of 0.61 both describe a toxin population with two kinds of site. The time course is consistent with the way the toxin was applied. The AFB_1 solution distributed over the grain in acetonitrile partly dries as a deposit on exposed kernel surfaces, where it meets the flux of reactive species directly and is removed within minutes. Part of the solution is carried by the solvent into the germ end, the crease and surface pores before it evaporates, and toxin held there is shaded by the kernel and by neighbouring kernels, while the organic matrix consumes short-lived radicals before they reach it. This partition, fast surface deposit and slow penetrated toxin, is the mechanism the two-fraction fit describes; the distribution of toxin within the kernels was not measured. Degradation of mycotoxins embedded in fungal culture extracts is slower than that of the pure compounds (ten Bosch et al. 2017), and corona-discharge treatment reduced AFB_1 more extensively on glass slides than in spiked rice and wheat (Puligundla et al. 2020). On corn, high-voltage plasma produced a logistic, non-log-linear course (Shi et al. 2017a). The levelling beyond 30 min follows from the same picture: once the accessible fraction is gone, further exposure acts on toxin that the discharge reaches with difficulty.

The chemistry of the first phase targets the parts of the AFB_1 molecule that carry its toxicity. Two structural features matter: the C8 = C9 vinyl ether double bond of the terminal dihydrofuran ring, which cytochrome P450 enzymes epoxidise (Kensler et al. 2011), and the coumarin lactone ring, which contributes to the planar, fluorescent chromophore. Under high-voltage atmospheric plasma, all six major products had lost the C8 = C9 double bond, and the lactone ring, cyclopentanone and methoxyl group were modified, so that the bioactivity of the treated toxin was substantially reduced (Shi et al. 2017b). Ozone adds across the vinyl ether double bond, hydroxyl and hydroperoxyl radicals add to it or epoxidise it, and further oxidation opens the lactone ring (Shi et al. 2017b; Hojnik et al. 2021b). Each of these pathways requires reactive species at the toxin, which is why accessibility sets the rate on grain. Kernel surfaces themselves showed slight oxidation under an indirect air plasma that removes AFB_1 (Hojnik et al. 2021a), which indicates that the toxin deposit is a preferred target of the reactive flux at the surface.

The chemistry of the accessible phase is well described for air plasmas. Structural studies show that both ozone and radicals act on AFB_1: under high-voltage atmospheric plasma, two of six major products were ozonolysis products and four arose from addition of H•, OH• and CHO• radicals or HO_2•-mediated epoxidation (Shi et al. 2017b), and under air plasma the rapid scission of the C8 = C9 vinyl bond removed cytotoxic and genotoxic potential (Hojnik et al. 2021b). Because this bond is the substrate for CYP-mediated formation of the 8,9-epoxide (Kensler et al. 2011), its loss removes the principal bioactivation route. Products were not identified in the present work, and these mechanistic conclusions rest on the cited studies.

Input current

Raising the input current from 2 to 4 A added 13.4 percentage points to the pooled reduction. A higher current lengthens the visible plume of this generator (Masunzu et al. submitted), so more of the grain

surface lies within the active discharge and the flux of reactive species to the accessible fraction rises. The effect of current is of the same order as the 10.9-point gain from extending exposure from 10 to 30 min, which makes current the more time-efficient lever within the stable operating range of the source. The two levers act on the same quantity, the supply of reactive species to the toxin, but in different ways. A higher current raises the rate of supply during the whole exposure, which accelerates removal of the accessible fraction and increases the share of the shielded fraction that the discharge can reach. A longer exposure at the same current extends the time over which the shielded fraction is attacked, and its return diminishes as the slow phase takes over. For a grain store this means that current should be set at the upper end of the stable range first, and exposure time then chosen to meet the target reduction.

Grain moisture and the reactive environment

The grain was treated at 13–14% moisture, the range typical of storage in tropical climates, and water at the kernel surface is part of the reactive environment. In humid air, electron impact on water vapour adds hydroxyl radicals to the species produced from oxygen and nitrogen (Misra et al. 2019). On corn treated with high-voltage plasma in a modified-atmosphere gas, aflatoxin degradation was greater at higher relative humidity (Shi et al. 2017a), consistent with a role for water-derived species. Standardising grain moisture before treatment therefore removes one source of run-to-run variation, and moisture is a candidate control variable for the shielded phase, which depends on the transport of reactive species to toxin held in the surface layers of the kernel.

Interpreting pooled marginal means

The current and time means are marginal means of a factorial design, each averaged over the levels of the other factors, including both electrode–sample distances and both cereals. They therefore describe the average response of the treatment series rather than any single condition, and they carry the advantage of averaging over the variation that a store operator will meet between grain lots and loading. The range of 60–85% across individual grain conditions shows the spread behind these averages. The upper end of this range, 85%, indicates what the best combination of settings delivers, and the regulatory analysis is therefore given for both the 30 min mean and the 85% value. The kinetic models inherit the same averaging: the Weibull shape parameter and the accessible fraction characterise the average time course and are robust indicators of its curvature, which all three means share.

If all maize eaten in a household were treated, the AFB_1 dose received from that maize would fall in the same proportion as the concentration. Applied to the median biomarker-based exposure of 105.5 ng/kg body weight per day in Tanzania (Kimanya et al. 2021), a 79.8% reduction corresponds to about 21.3 ng/kg body weight per day for the share of exposure carried by treated maize. The relation is linear, so the same proportional benefit applies across the exposure distribution, from its lower end of 15.0 ng/kg body weight per day to its upper end of 10,926.0 ng/kg body weight per day. At the upper end, however, the residual dose remains high, which again points to sorting and combined control for the most heavily contaminated grain.

Comparison with published plasma treatments

Published plasma treatments of aflatoxin on cereals, nuts and seeds are compared with the present result in Table 4. The 79.8% pooled 30 min mean and the 85% upper value on maize and wheat are of the same order as the 82% reached on corn after 10 min of high-voltage plasma (Shi et al. 2017a), above the 66% reported in maize with cold atmospheric plasma (Wielogorska et al. 2019), and close to the 82.6% reached on naturally contaminated maize after about 30 min of low-pressure nitrogen plasma at 189.8 W (Kamano et al. 2025). DBD treatment reduced AFB_1 in oat by 82% in 6 min at 37 W (Dousti et al. 2024), argon DBD reduced it in sesame by 68.6% in 8 min at 56 W (Ghaani et al. 2025), and 1000 W plasma reduced aflatoxins in hazelnuts by more than 70% in 12 min (Siciliano et al. 2016). An indirect surface barrier discharge removed AFB_1 completely from contaminated corn kernels (Hojnik et al. 2021a). The studies differ in contamination route, toxin level, gas, pressure and power, so the comparison establishes order of magnitude. Within that range, the present source reaches comparable reductions with ambient air at atmospheric pressure, without a gas supply or vacuum system.

Table 4
Published plasma treatments of aflatoxins on cereals, nuts and seeds compared with the present work (literature data)

Source	Gas and pressure	Power or setting	Time	Matrix	Reduction	Reference
High-voltage atmospheric cold plasma	Air, RH 40%, atmospheric	High voltage	1; 10 min	Corn	62%; 82% (aflatoxin)	Shi et al. (2017a)
Cold atmospheric plasma	Atmospheric	–	–	Maize	Up to 66% (AFB_1)	Wielogorska et al. (2019)
Low-temperature nitrogen plasma	Nitrogen, 0.98 Pa	189.8 W	1793 s	Naturally contaminated maize	82.6% (aflatoxin)	Kamano et al. (2025)
Indirect surface barrier discharge	Ambient air, atmospheric	–	–	Spiked corn kernels	Complete (AFB_1)	Hojnik et al. (2021a)
Dielectric barrier discharge	Atmospheric	37 W	6 min	Oat	82% (AFB_1)	Dousti et al. (2024)
Dielectric barrier discharge	Argon, atmospheric	56 W	8 min	Sesame	68.6% (AFB_1)	Ghaani et al. (2025)
Cold atmospheric plasma	Nitrogen–oxygen mixtures	1000 W	12 min	Hazelnut	> 70% (AFB_1, total)	Siciliano et al. (2016)
Tesla-coil point discharge (this work)	Ambient air, atmospheric	2–4 A input current	10–30 min	Spiked maize and wheat	68.9–79.8% (pooled means); 60–85% (range)	This work

Values as reported in the cited studies; "–", not specified in the source summary.

The published studies also differ in how they express treatment intensity, which limits direct comparison. Some report electrical power in watts (Dousti et al. 2024; Ghaani et al. 2025; Kamano et al. 2025; Siciliano et al. 2016), others voltage or exposure time alone (Shi et al. 2017a), and the present study reports input current and time, the controllable parameters of its generator. A common basis, such as energy delivered per unit mass of grain, would allow sources to be compared on equal terms. The study on naturally contaminated maize (Kamano et al. 2025) is the closest benchmark for the next step of the present work, because it measures reduction of toxin produced by the fungus within the grain rather than toxin added to its surface.

Routes to compliance

The regulatory analysis converts the time course into a decision rule for toxin at or near the kernel surface. Grain at up to about 25 µg/kg, which covers the median of contaminated home-stored maize in rural Tanzania (Kimanya et al. 2008), reaches the East African limit after one 30 min treatment at these settings. Heavily contaminated grain requires a reduction of 96.8–99.8%, which the shielded fraction prevents a single exposure from reaching. Three routes follow from the biphasic course. First, exposing more kernel surface, by agitation or by moving the grain in a thin layer under the electrode, converts shielded toxin into accessible toxin; stirring during treatment increased aflatoxin degradation in corn under high-voltage plasma (Shi et al. 2017a). Second, repeated short treatments with remixing between them exploit the rapid first phase several times. Third, combining sorting, which removes visibly damaged and heavily contaminated kernels (Karlovsky et al. 2016), with a plasma polishing step brings the starting level into the range that one treatment can handle. Each route targets the shielded fraction identified by the kinetic models.

In the post-harvest chain, the plasma step sits after drying and cleaning and before storage or milling. Drying brings grain to the moisture range used here, cleaning removes dust and fines that would shade kernels, and sorting removes visibly mouldy kernels that carry the highest toxin loads (Karlovsky et al. 2016). A 50 g batch at a 2 cm electrode–sample distance defines the laboratory scale of this study; the regulatory analysis applies per batch and is independent of batch size, provided each kernel receives the same exposure. For a cooperative store, the analysis therefore gives a sampling-based rule: lots whose measured AFB_1 lies within the compliance band are treated directly, and lots above it are sorted first and then treated, with a post-treatment check against the limit.

The European framework already distinguishes maize destined for sorting or other physical treatment, for which it allows 5 µg/kg AFB_1 and 10 µg/kg total aflatoxins before treatment, from cereals for direct human consumption at 2 and 4 µg/kg (European Commission 2023). A validated plasma step would sit naturally in the first category, and the present data show the scale of reduction it can contribute: a 30 min treatment brings grain at the pre-treatment AFB_1 limit of 5 µg/kg down to about 1.0 µg/kg, below the direct-consumption limit. For the East African standard, which sets single limits for grain (East African Community 2011), the analysis identifies the contamination band, up to about 25 µg/kg, within which plasma treatment alone restores compliance. Because exposure to aflatoxin through maize scales with the concentration consumed, a reduction of 79.8% at this band lowers the dietary AFB_1 dose from that grain in the same proportion, which is the outcome that matters for the liver-cancer burden attributed to aflatoxin in Tanzania (Kimanya et al. 2021).

Contribution

The study adds three elements to the plasma literature on aflatoxin in cereals. It reports reduction on maize and wheat from an atmospheric-pressure source that uses room air and mains power, with effect sizes and confidence intervals for current and exposure time. It describes the time course quantitatively,

with a Weibull shape parameter and a two-fraction partition that separate surface-accessible from shielded toxin and locate the ceiling of a single exposure. It converts the result into the starting-concentration band that one treatment brings within the East African and European limits, and sets that band against contamination measured in Tanzanian households. Together, these elements turn a laboratory reduction into a decision a grain store can act on: treat grain in the lower band directly, and route heavily contaminated grain through agitation, repeated passes or sorting before the plasma step.

Scope

The kinetic parameters describe pooled marginal means over input current, electrode–sample distance and the two cereals, and they characterise the shape of the time course for this source and these settings. The results apply to toxin at or near the kernel surface. In naturally contaminated grain, fungal toxin is distributed through the kernel tissue together with other aflatoxins and viable fungi (Kamano et al. 2025), so the compliance cut-offs derived here are upper bounds for a single treatment, and naturally contaminated grain is the next test. Treatments are specified by input current, distance and time, the controllable parameters of the generator. Condition-level data for each cereal, identification of degradation products, toxicological testing of treated grain and trials on naturally contaminated maize are the next steps. Under these conditions, ambient-air plasma serves as a compliance step for moderately contaminated maize and wheat and as one stage of combined control for heavily contaminated lots.

Declarations

Source of funding

N.M.'s postgraduate studies were sponsored by the Ministry of Education, Science and Technology, Tanzania; the research received no other specific funding.

Conflicts of interest

Conflicts of interest: None. No patent has been filed on the generator described.

Ethics approval

Not applicable: the study did not involve human participants or animals. The work complied with the laws of the United Republic of Tanzania.

Author Contribution

N.M. and J.R. conceived the study. N.M., M.C. and J.R. designed the methodology. N.M. built the generator, carried out the experiments, curated and analysed the data, prepared the figures and wrote the original draft. M.C. and J.R. supervised the work and reviewed and edited the manuscript. N.M acquired funding. All authors reviewed and approved the final manuscript.

Acknowledgements

The authors thank Mwalimu Julius K. Nyerere University of Agriculture and Technology for granting N.M. study leave.

Data Availability

The summary data analysed in this study (means, standard deviations and 95% confidence intervals) are given in Table 1; replicate data are available from the corresponding author on reasonable request.

References

1. Dousti M, Bashiry M, Zohrabi P, Siahpoush V, Ghaani A, Abdolmaleki K (2024) The effect of dielectric barrier discharge (DBD) cold plasma treatment on the reduction of aflatoxin B1 and the physicochemical properties of oat. Appl Food Res 4:100515. https://doi.org/10.1016/j.afres.2024.100515
2. East African Community (2011) EAS 2:2011 Maize Grains—Specification, 3rd edn. East African Community, Arusha, Tanzania
3. European Commission (2023) Commission Regulation (EU) 2023/915 of 25 April 2023 on maximum levels for certain contaminants in food and repealing Regulation (EC) 1881/2006. Off J Eur Union L 119:103–157. http://data.europa.eu/eli/reg/2023/915/oj
4. European Committee for Standardization (2007) EN 14123:2007 Foodstuffs—Determination of aflatoxin B1 and the sum of aflatoxin B1, B2, G1 and G2 in hazelnuts, peanuts, pistachios, figs, and paprika powder—High performance liquid chromatographic method with post-column derivatisation and immunoaffinity column clean up. CEN, Brussels, Belgium
5. Gavahian M, Cullen PJ (2020) Cold plasma as an emerging technique for mycotoxin-free food: efficacy, mechanisms, and trends. Food Rev Int 36:193–214. https://doi.org/10.1080/87559129.2019.1630638
6. Ghaani A, Bashiry M, Zohrabi P, Siahpoush V, Mollakhalili Meybodi N, Dousti M, Abdolmaleki K (2025) Investigating the effect of dielectric barrier discharge cold plasma on the aflatoxin removal and the physicochemical properties of sesame seeds. Sci Rep 15:32052. https://doi.org/10.1038/s41598-025-17731-6
7. Gichohi-Wainaina WN, Kimanya M, Muzanila YC, Kumwenda NC, Msere H, Rashidi M, Mponda O, Okori P (2023) Aflatoxin contamination, exposure among rural smallholder farming Tanzanian mothers and associations with growth among their children. Toxins 15:257. https://doi.org/10.3390/toxins15040257
8. Hojnik N, Cvelbar U, Tavčar-Kalcher G, Walsh JL, Križaj I (2017) Mycotoxin decontamination of food: cold atmospheric pressure plasma versus classic decontamination. Toxins 9:151. https://doi.org/10.3390/toxins9050151

9. Hojnik N, Modic M, Žigon D, Kovač J, Jurov A, Dickenson A, Walsh JL, Cvelbar U (2021a) Cold atmospheric pressure plasma-assisted removal of aflatoxin B1 from contaminated corn kernels. Plasma Process Polym 18:2000163. https://doi.org/10.1002/ppap.202000163
10. Hojnik N, Modic M, Walsh JL, Žigon D, Javornik U, Plavec J, Žegura B, Filipič M, Cvelbar U (2021b) Unravelling the pathways of air plasma induced aflatoxin B1 degradation and detoxification. J Hazard Mater 403:123593. https://doi.org/10.1016/j.jhazmat.2020.123593
11. IARC Working Group on the Evaluation of Carcinogenic Risks to Humans (2012) Chemical Agents and Related Occupations. IARC Monographs on the Evaluation of Carcinogenic Risks to Humans, vol 100. F. International Agency for Research on Cancer, Lyon, France
12. Javed M, Cao W, Tang L, Keener KM (2025) A review of decontamination of Aspergillus spp. and aflatoxin control for grains and nuts with atmospheric cold plasma. Toxins 17:129. https://doi.org/10.3390/toxins17030129
13. Kamano HM, Okoth MW, Kogi-Makau W, Kuloba PW, Owade JO, Njage PMK (2025) Optimization of low-temperature nitrogen plasma in reducing fungi and aflatoxin human exposure through maize. Sci Rep 15:11707. https://doi.org/10.1038/s41598-025-95153-0
14. Karlovsky P, Suman M, Berthiller F, De Meester J, Eisenbrand G, Perrin I, Oswald IP, Speijers G, Chiodini A, Recker T, Dussort P (2016) Impact of food processing and detoxification treatments on mycotoxin contamination. Mycotoxin Res 32:179–205. https://doi.org/10.1007/s12550-016-0257-7
15. Kensler TW, Roebuck BD, Wogan GN, Groopman JD (2011) Aflatoxin: a 50-year odyssey of mechanistic and translational toxicology. Toxicol Sci 120(Suppl 1):S28–S48. https://doi.org/10.1093/toxsci/kfq283
16. Khlangwiset P, Shephard GS, Wu F (2011) Aflatoxins and growth impairment: a review. Crit Rev Toxicol 41:740–755. https://doi.org/10.3109/10408444.2011.575766
17. Kimanya ME, De Meulenaer B, Tiisekwa B, Ndomondo-Sigonda M, Devlieghere F, Van Camp J, Kolsteren P (2008) Co-occurrence of fumonisins with aflatoxins in home-stored maize for human consumption in rural villages of Tanzania. Food Addit Contam Part A 25:1353–1364. https://doi.org/10.1080/02652030802112601
18. Kimanya ME, Routledge MN, Mpolya E, Ezekiel CN, Shirima CP, Gong YY (2021) Estimating the risk of aflatoxin-induced liver cancer in Tanzania based on biomarker data. PLoS ONE 16:e0247281. https://doi.org/10.1371/journal.pone.0247281
19. Larson DA (1992) Analysis of variance with just summary statistics as input. Am Stat 46:151–152. https://doi.org/10.1080/00031305.1992.10475872
20. Liu Y, Wu F (2010) Global burden of aflatoxin-induced hepatocellular carcinoma: a risk assessment. Environ Health Perspect 118:818–824. https://doi.org/10.1289/ehp.0901388
21. Mafart P, Couvert O, Gaillard S, Leguerinel I (2002) On calculating sterility in thermal preservation methods: application of the Weibull frequency distribution model. Int J Food Microbiol 72:107–113. https://doi.org/10.1016/S0168-1605(01)00624-9

22. Misra NN, Yadav B, Roopesh MS, Jo C (2019) Cold plasma for effective fungal and mycotoxin control in foods: mechanisms, inactivation effects, and applications. Compr Rev Food Sci Food Saf 18:106–120. https://doi.org/10.1111/1541-4337.12398
23. Park BJ, Takatori K, Sugita-Konishi Y, Kim I-H, Lee M-H, Han D-W, Chung K-H, Hyun SO, Park J-C (2007) Degradation of mycotoxins using microwave-induced argon plasma at atmospheric pressure. Surf Coat Technol 201:5733–5737. https://doi.org/10.1016/j.surfcoat.2006.07.092
24. Puligundla P, Lee T, Mok C (2020) Effect of corona discharge plasma jet treatment on the degradation of aflatoxin B1 on glass slides and in spiked food commodities. LWT 124:108333. https://doi.org/10.1016/j.lwt.2019.108333
25. Shi H, Ileleji K, Stroshine RL, Keener K, Jensen JL (2017a) Reduction of aflatoxin in corn by high voltage atmospheric cold plasma. Food Bioprocess Technol 10:1042–1052. https://doi.org/10.1007/s11947-017-1873-8
26. Shi H, Cooper B, Stroshine RL, Ileleji KE, Keener KM (2017b) Structures of degradation products and degradation pathways of aflatoxin B1 by high-voltage atmospheric cold plasma (HVACP) treatment. J Agric Food Chem 65:6222–6230. https://doi.org/10.1021/acs.jafc.7b01604
27. Siciliano I, Spadaro D, Prelle A, Vallauri D, Cavallero M, Garibaldi A, Gullino ML (2016) Use of cold atmospheric plasma to detoxify hazelnuts from aflatoxins. Toxins 8:125. https://doi.org/10.3390/toxins8050125
28. ten Bosch L, Pfohl K, Avramidis G, Wieneke S, Viöl W, Karlovsky P (2017) Plasma-based degradation of mycotoxins produced by Fusarium, Aspergillus and Alternaria species. Toxins 9:97. https://doi.org/10.3390/toxins9030097
29. Trucksess MW, Stack ME, Nesheim S, Page SW, Albert RH, Hansen TJ, Donahue KF (1991) Immunoaffinity column coupled with solution fluorometry or liquid chromatography postcolumn derivatization for determination of aflatoxins in corn, peanuts, and peanut butter: collaborative study. J AOAC Int 74:81–88. https://doi.org/10.1093/jaoac/74.1.81
30. Virtanen P, Gommers R, Oliphant TE, Haberland M, Reddy T, Cournapeau D, Burovski E, Peterson P, Weckesser W, Bright J et al (2020) SciPy 1.0: fundamental algorithms for scientific computing in Python. Nat Methods 17:261–272. https://doi.org/10.1038/s41592-019-0686-2
31. Wielogorska E, Ahmed Y, Meneely J, Graham WG, Elliott CT, Gilmore BF (2019) A holistic study to understand the detoxification of mycotoxins in maize and impact on its molecular integrity using cold atmospheric plasma treatment. Food Chem 301:125281. https://doi.org/10.1016/j.foodchem.2019.125281

Figures

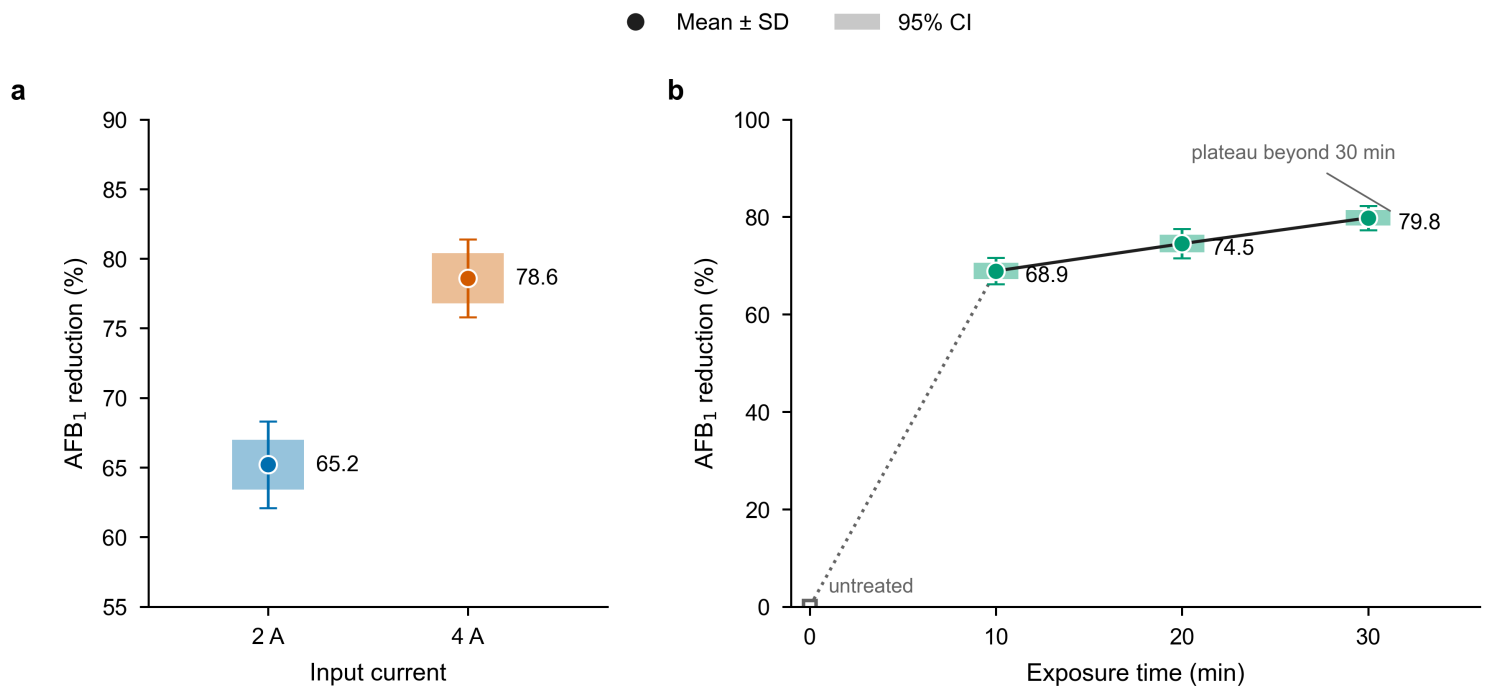


Figure 1

AFB_1 reduction on spiked maize and wheat. (**a**) Effect of input current, pooled over exposure time and electrode–sample distance. (**b**) Effect of exposure time, pooled over input current and distance; the square marks the untreated control and the annotation the levelling of reduction beyond 30 min. Points show mean ± SD; shaded boxes show 95% CI

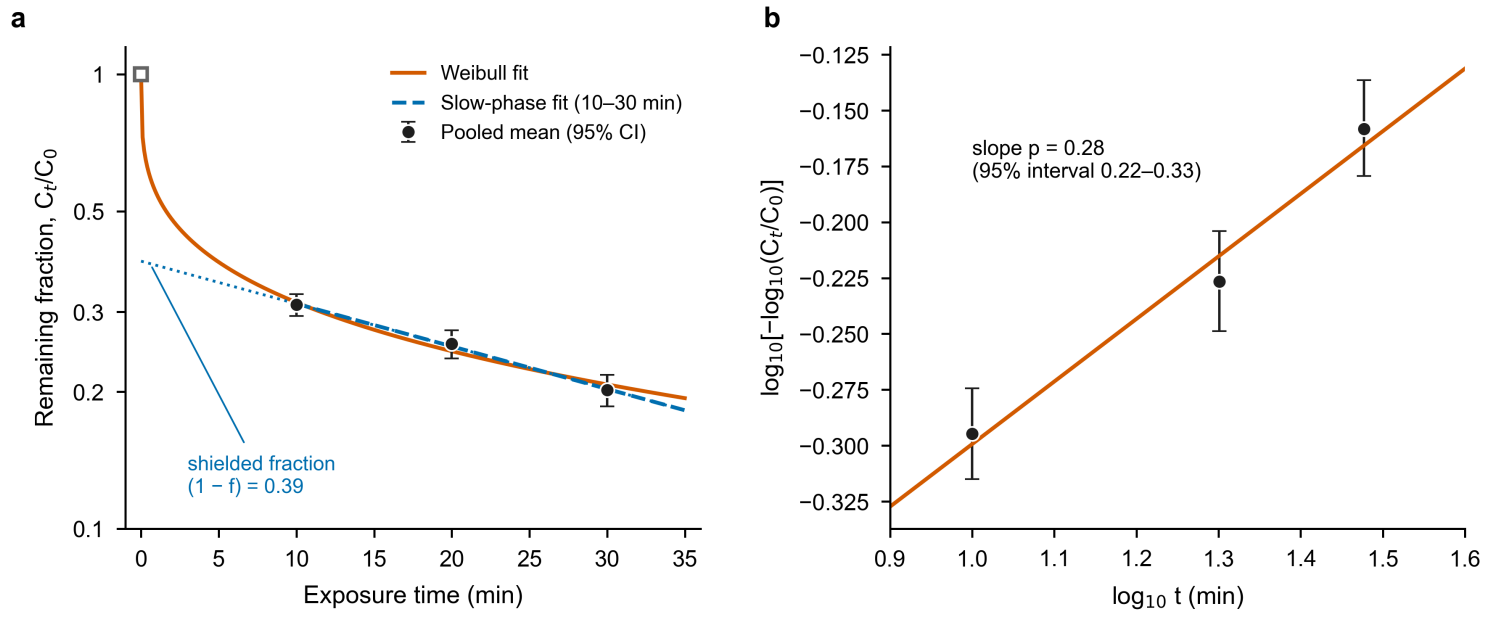


Figure 2

Time course of AFB_1 reduction on spiked grain, fitted to the pooled time means. (**a**) Remaining fraction C_t/C_0 (log scale) with the Weibull fit and the slow-phase fit of the two-fraction model over 10–30 min; the

dotted extension to t = 0 gives the shielded fraction (1 − f). Points show means with 95% CI. (**b**) Weibull linearisation; the slope is the shape parameter p

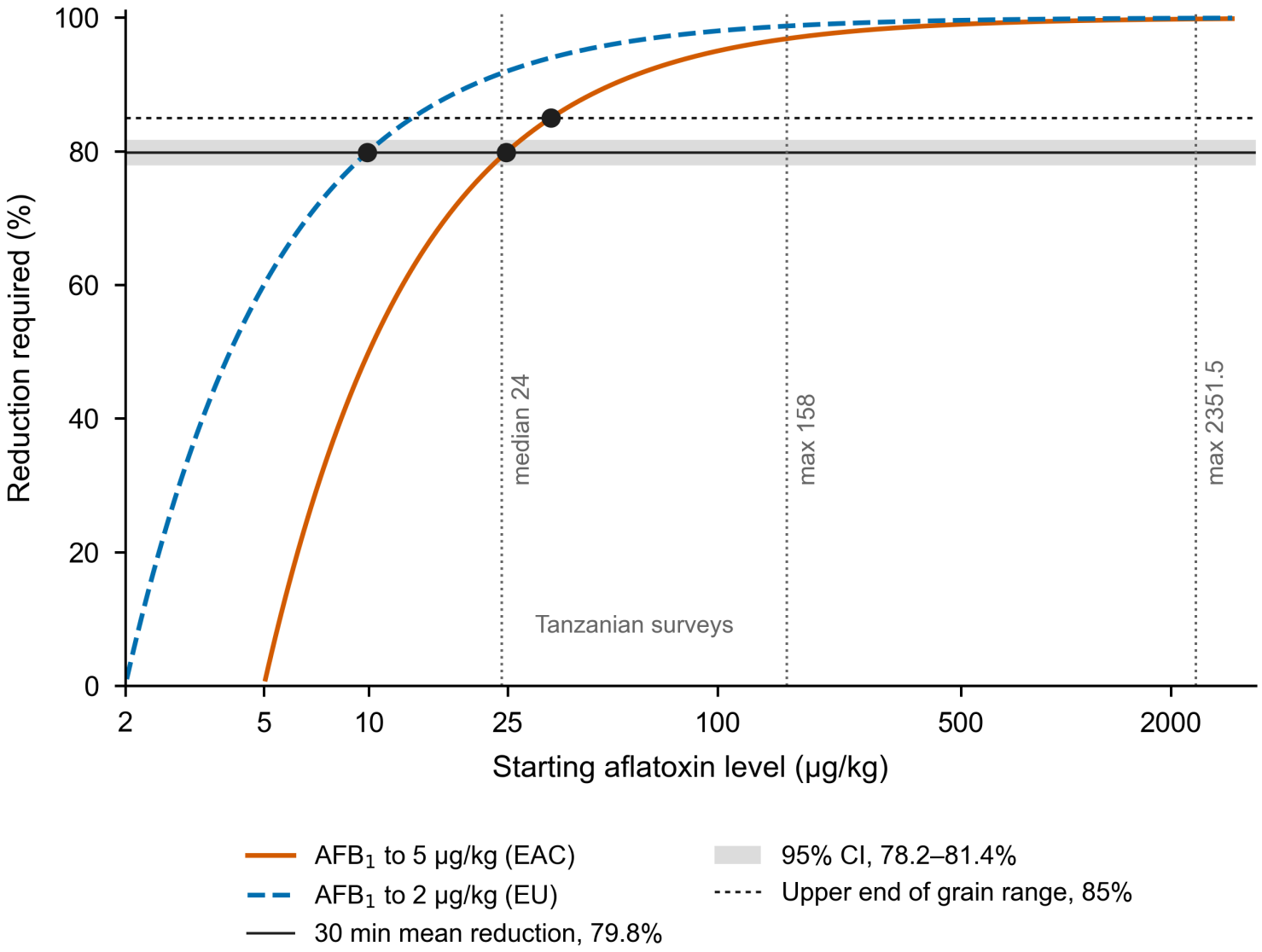


Figure 3

Reduction required to bring grain to the East African (EAC, 5 µg/kg) and European (EU, 2 µg/kg) AFB_1 limits as a function of starting level, set against the 30 min mean reduction (line, with 95% CI band) and the upper end of the grain range (dotted). Filled circles mark the break-even starting levels; vertical lines mark Tanzanian survey values